Document downloaded from:

http://hdl.handle.net/10251/103730

This paper must be cited as:

Llopis-Lorente, A.; De Luis-Fernández, B.; García-Fernández, A.; Diez, P.; Sánchez, A.; Marcos Martínez, MD.; Villalonga, R.... (2017). Au-Mesoporous silica nanoparticles gated with disulfide-linked oligo(ethylene glycol) chains for tunable cargo delivery mediated by an integrated enzymatic control unit. Journal of Materials Chemistry B. 5(33):6734-6739. doi:10.1039/c7tb02045g

The final publication is available at

http://doi.org/10.1039/c7tb02045g

Copyright The Royal Society of Chemistry

Additional Information

Journal Name

COMMUNICATION

Au-Mesoporous Silica Nanoparticles Gated with Disulfide-Linked Oligo(Ethylene Glycol) Chains for Tunable Cargo Delivery Mediated by an Integrated Enzymatic Control Unit

Received 00th January 20xx,
Accepted 00th January 20xx

DOI: 10.1039/x0xx00000x

www.rsc.org/

Antoni Llopis-Lorente,[a,b,c] Beatriz de Luis,[a,b,c] Alba García-Fernández,[a,b,c] Paula Díez,[d] Alfredo Sánchez,[d] M. Dolores Marcos,[a,b,c] Reynaldo Villalonga,*[d] Ramón Martínez-Máñez*[a,b,c] and Félix Sancenón[a,b,c]

We report a delivery system based on Au-mesoporous silica (MS) nanoparticles functionalized with acetylcholinesterase on the Au face as a control unit and with disulfide-containing oligo(ethylene glycol) chains on the MS face as caps. The control unit handles the chemical information in the environment (the presence of acetylthiocholine or enzyme inhibitors) that results in a tuned cargo delivery from the nanocarrier. The nanodevice displayed an enhanced cargo delivery in cancer cells (safranin O and doxorubicin) in the presnece of acetylthiocholine.

In recent years, the development of smart delivery systems able to release their cargo upon application of specific stimuli has attracted much attention due to their potential application in the biomedical and sensing fields.[1] Systems based on liposomes, inorganic scaffolds and polymeric nanoparticles having different size, structure, surface and delivery properties have been reported.[2] In addition, researchers are currently developing active nanomotors using enzymes as future nanovehicles, and some examples are already available.[3] Among potential drug nanocarriers, mesoporous silica (MS) supports are especially appealing because of their unique properties, such as chemical stability, high loading capacity, low cost and biocompatibility.[4] Gated MS supports for cargo delivery usually contain two subunits: (i) a porous scaffold in which a cargo is loaded and (ii) molecular, supramolecular or bio-molecular ensembles, placed on the external surface of the loaded solid, capable of being "opened" or "closed" on-command in order to control payload delivery from pores. In line with this concept, examples of gated MS supports responsive to physical (light, temperature, magnetic fields, ultrasounds), chemical (anions, cations, neutral molecules, redox-active species and pH) and biochemical (such as enzymes, DNA and antibodies) stimuli have been reported.[5]

Inside this area of gated materials, we have recently reported the design of more sophisticated nanodevices for delivery applications based on Janus nanoparticles with Au and MS on opposite faces.[6] This allows the immobilization of enzymes on the Au face (control unit) and molecular/supramolecular gates on the MS face. The role of the "control unit" is to handle chemical information (input) of the environment and transform it into new molecules that control the state of the gate (open or closed) (see Scheme 1). Such systems have been used in complex communication networks.[5h,6c] Moreover, this expands the possibilities for the construction of smart delivery systems since enzymes can be chosen to recognize a large number of different specific substrates and produce a certain stimulus, through an enzyme-mediated process, able to open the gated ensemble. As far as we know, very few examples of gated Janus Au-MS nanoparticles have been reported and both are based on enzyme-mediated commutation of pH-responsive molecular gates.[6]

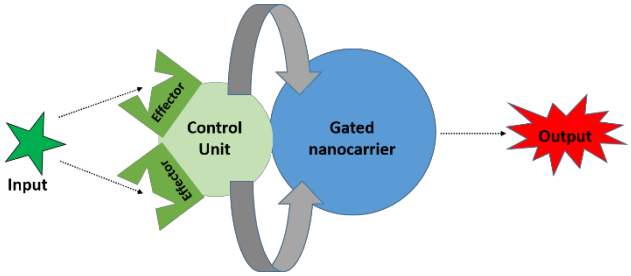

Scheme 1. Representation of a Janus Au-MS nanodevice containing a control unit that regulates delivery in the gated MS face.

With the aim of opening new directions towards the construction of smart delivery systems, we report herein the first example of an enzyme-controlled Janus Au-MS nanodevice in which delivery is driven by a thiol-exchange

[a] Instituto de Reconocimiento Molecular y Desarrollo Tecnológico (IDM), Unidad Mixta Universidad Politécnica de Valencia-Universidad de Valencia (Spain)
[b] Departamento de Química, Universidad Politécnica de Valencia. Camino de Vera s/n, 46022, Valencia (Spain). E-mail: rmaez@qim.upv.es
[c] CIBER de Bioingeniería, Biomateriales y Nanomedicina (CIBER-BBN) (Spain)
[d] Nanosensors & Nanomachines Group, Department of Analytical Chemistry, Faculty of Chemistry, Complutense University of Madrid, 28040 Madrid (Spain). E-mail: rvillalonga@quim.ucm.es
Electronic Supplementary Information (ESI) available: Experimental procedures and Materials Characterisation. See DOI: 10.1039/x0xx00000x

Please do not adjust margins

redox mechanism. Additionally, we also show that cargo release can be modulated by the presence of certain substances. Usually gated nanodevices exhibited a simple delivery upon application of a triggering stimulus. However, in our designed system, the control unit is able to detect the presence of certain chemicals in the solution (enzyme inhibitors) and tune cargo delivery accordingly.

Scheme 2 illustrates the design and operation of the system. The enzyme acetylcholinesterase was immobilized on the Au face of the Janus Au-MS nanoparticles. The MS face was loaded with a suitable cargo (safranin O) and its external surface was functionalized with disulfide-containing oligo(ethylene glycol) chains (SS-OEG) which act as molecular gates. The Au side (control unit) was functionalized with acetylcholinesterase that is able to detect the presence of acetylthiocholine, a derivative of the neurotransmitter acetylcholine.[7] In particular, the hydrolysis of acetylthiocholine[8] by the enzyme produces thiocholine that cleavages the disulfide bond on the MS face resulting in pore opening and payload release. Moreover, the nanodevice is also sensitive to the presence of diisopropyl fluorophosphate (DFP) which regulates enzyme activity and consequently also cargo delivery from the MS face.

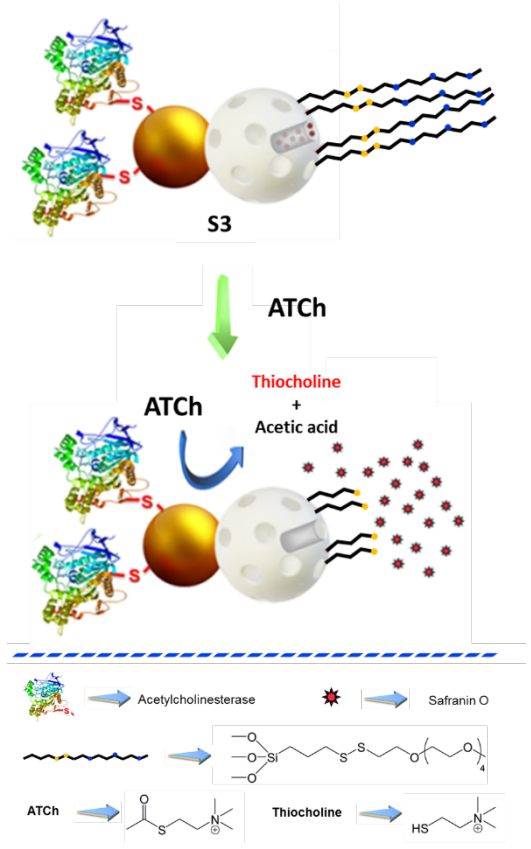

Scheme 2. Representation of the performance of the nanodevice **S3**. The "control unit" (Au face is functionalized with acetylcholinesterase, which directs the cargo delivery form the mesoporous face in the presence of acetylthiocholine (ATCh).

In order to prepare the nanodevice, first MS nanoparticles were obtained by hydrolysis and condensation of tetraethyl orthosilicate in basic media using cetyltrimethylammonium bromide as a template. The surfactant was then removed by calcination in air at high temperature which yield the starting mesoporous support. In a second step, gold nanoparticles were synthesised by reduction of Au(III) with sodium citrate based on the Turkevich-Frens method.[9] Next, MS nanoparticles were confined at the interface of a Pickering emulsion between paraffin and an aqueous face in order to achieve its partial functionalization with (3-mercaptopropyl)trimethoxysilane on which Au nanoparticles were attached by the formation of S-Au bonds. The paraffin wax was removed by washing with $CHCl_3$ which yield the initial Janus Au-MS nanoparticles (**S1**). In a further step, the pores of the MS face were loaded with safranin O by stirring overnight at room temperature a suspension of the nanoparticles in an aqueous solution of the dye. Next, the Au surface was functionalized with 3-mercaptopropionic acid, which was attached by the formation of Au-S bonds. Afterward, an excess of (3-mercaptopropyl)trimethoxysilane was added to functionalize the mesoporous surface and the thiol-functionalized solid was further reacted with 2,2-dipyridyl disulfide. Then, substitution of dipyridyl groups by reaction with O-(2-mercaptoethyl)-O-methyl-hexa(ethylene glycol) (SS-OEG) allowed the capping of the mesoporous scaffold yielding the nanoparticles **S2**. Finally, the enzyme acetylcholinesterase was immobilized by coupling lysine residues in the enzyme with the carboxylic groups on the gold surface via the use of N-hydroxysuccinimide (NHS) and ethyl(dimethylaminopropyl) carbodiimide (EDC).[10] This process finally yielded **S3** nanoparticles (see Scheme 3) which were kept wet in the refrigerator until use. Nanoparticles similar to **S3,** but loaded with the cytotoxic agent doxorubicin, were also prepared (**$S3_{DOX}$**, see Supporting Info for details).

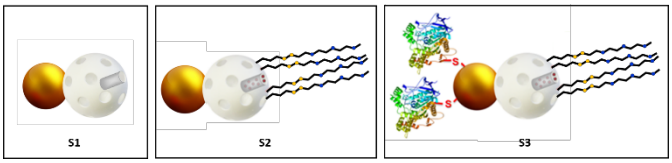

Scheme 3. Representation of the Janus Au-MS nanoparticles (**S1**), capped nanoparticles (**S2**) and enzyme-functionalized nanodevice (**S3**).

Solids were characterized using standard procedures (see Supporting Information). The mesoporous morphology of the MS nanoparticles (diameter of ca. 70-100 nm) as well as the presence of the Au nanoparticles (diameter of ca. 20-25 nm) in Au-MS colloids was confirmed by transmission electron microscopy (TEM) analysis (see Figure 1 and Figure SI-1 for additional images). The powder X-ray diffraction (PXRD) pattern of the starting MS nanoparticles showed the mesoporous characteristic reflection peak (100) around 2.4° (see Figure 1). The preservation of this typical peak in **S1** and **S2** clearly confirms that the surface functionalization and cargo loading processes did not damage the mesoporous scaffolding.

This journal is © The Royal Society of Chemistry 20xx

Please do not adjust margins

Moreover, the diffraction pattern at high angles for Janus colloids showed the cubic gold nanocrystals characteristic (111), (200), (220), and (311) peaks,[11] confirming the Au-MS architecture observed by TEM (see also Figure 1). N_2 adsorption-desorption isotherms of starting MS and **S1** showed an adsorption step at intermediate P/P_0 values (0.1-0.3) which indicates the presence of empty pores (see Figure SI-2). BET specific surface area,[12] BJH pore volumes[13] and pore sizes were calculated and are summarized in Table SI-1. Moreover, contents of safranin O and SS-OEG groups in **S2** were determined by elemental analysis (see Table SI-2), giving values of 52.6 and 137 mg per gram of solid, respectively. Furthermore, the activity of immobilized enzyme on the final nanodevice **S3** was determined to be 797 $U \cdot g^{-1}$, that corresponds to 3.5 $mg \cdot g^{-1}$ (see Figure SI-3). Moreover, TEM-EDX mapping of the gold side of the nanodevice shows that this area was rich in sulphur atoms (see Supporting Information), thus confirming the preferential localization of the enzyme in the gold face.

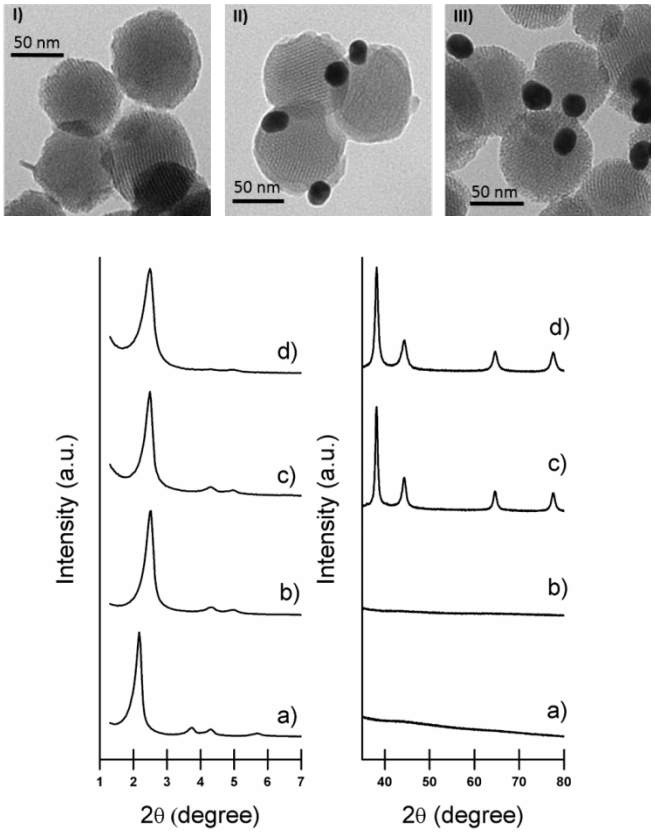

Figure 1. Top: TEM images of (I) calcined mesoporous silica, (II) Janus Au-MS nanoparticles (**S1**) and (III) capped nanoparticles (**S2**). Down: PXRD of (a) as-made mesoporous silica, (b) calcined mesoporous silica, (c) Janus Au-MS nanoparticles (**S1**) and (d) capped nanoparticles (**S2**) at low (left) and high (right) angles.

In order to test the ability of the nanodevice to recognize acetylthiocholine, we brought **S3** to a concentration of 0.9 $mg \cdot mL^{-1}$ in aqueous solution at pH 7.5 (50 mM sodium phosphate buffer) in the absence and presence of acetylthiocholine (1 mM). Aliquots were taken at scheduled times, centrifuged to remove nanoparticles, and cargo release was evaluated by measuring the emission band of safranin O at 585 nm (λ_{exc} = 520 nm). Figure 2 shows payload delivery kinetics. In the absence of acetylchiocholine, dye release from **S3** was negligible. However, presence of acetylthiocholine induced pore opening and a subsequent remarkable cargo delivery in less than one hour. In addition, we also carried out experiments in 50 mM sodium phosphate buffer at different relevant pHs, in simulated blood plasma and in PBS (see Supporting Information for details) and in all these cases a similar behaviour was observed (see Figure 3). The observed payload release is attributed to the "detection" of acetylthiocholine by acetylcholinesterase in the control unit. The enzyme transforms acetylthiocholine into thiocholine, which induced cleavage of disulfide bonds in SS-OEG on the MS face, finally resulting in uncapping of the pores and cargo delivery. Thiocholine is able to break disulphide bonds via a thiol-disulfide interchange reaction.[14] This reaction consists on a nucleophilic substitution of a thiol in disulfides with another thiol from a different molecule and plays an important role in biochemistry.

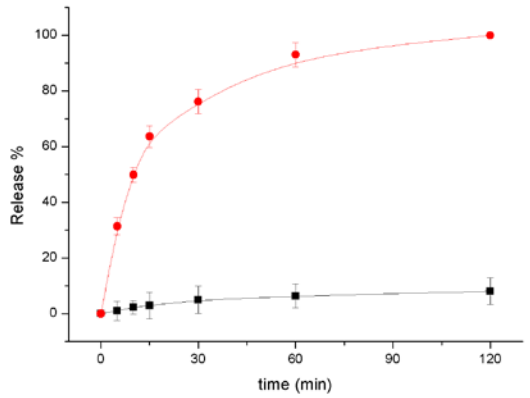

Figure 2. Normalized cargo release from **S3** determined by measuring safranin O fluorescence at 585 nm (λ_{exc} = 520 nm) versus time in aqueous solution (50 mM sodium phosphate buffer, pH 7.5) in the absence (black) and presence (red) of acetylthiocholine 1 mM. Error bars from three independent experiments.

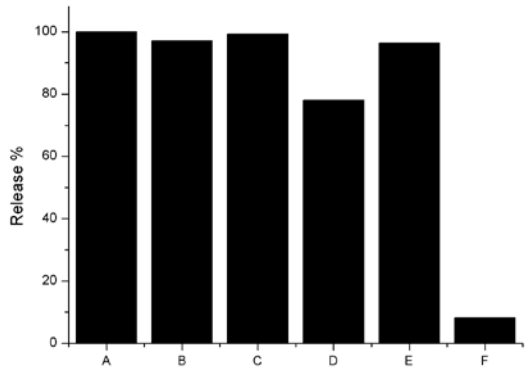

Figure 3. Normalized cargo release from **S3** determined by measuring safranin O fluorescence at 585 nm (λ_{exc} = 520 nm) under different conditions after 120 min. From left to right: in the presence of ATCh 1 mM in 50 mM sodium phosphate

Please do not adjust margins

buffer at pH 7.5 (A), pH 8.5 (B) and pH 6.5 (C); in the presence of ATCh 1 mM in simulated body plasma (D) and PBS (E) and in the absence of ATCh in PBS (F).

In order to validate the proposed gating mechanism, we carried out additional control experiments. First, the response of **S3** in the presence of acetylcholine was studied. Acetylcholine is also hydrolyzed by the enzyme resulting in the formation of choline and acetic acid.[8] In this case, the release from **S3** in the presence of acetylcholine was negligible since the enzymatic process does not yield thiocholine and therefore the MS face remained capped (Figure 4). Release experiments in the presence of sodium iodide showed that the anion iodide (we used acetylthiocholine iodide for the release experiments in Figure 2) had no effect in the response of **S3** (Figure 4). Moreover, the response of the capped solid **S2** (without enzyme) in the presence of acetylthiocholine resulted in no delivery demonstrating the key role played by the enzyme in the "control unit". The fact that **S3** is able to deliver the cargo in the presence of acetylthiocholine and not with acetylcholine points out how enzymes and molecular gates can be assembled on Janus nanoparticles to operate synergistically and recognize small differences on molecular structure.

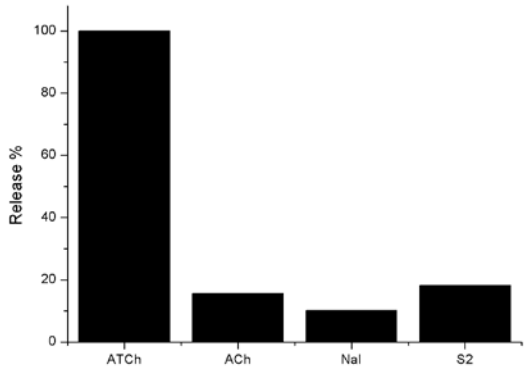

Figure 4. Normalized cargo release from **S3** in aqueous solution (50 mM sodium phosphate buffer, pH 7.5) in the presence of acetylthiocholine (ATCh), acetylcholine (ACh), and sodium iodide and from **S2** (without enzyme) in the presence of ATCh after 120 min.

Encouraged by these findings, we tested in a further step if delivery from **S3** could also be tuned by the presence of enzyme inhibitors. Diisopropyl fluorophosphate (DFP) is a known acetylcholinesterase inhibitor which is used in neuromedicine, also as a pesticide and as a nerve agent simulant.[15] In the presence of DFP, acetylcholinesterase is phosphorylated at the active site, and accordingly, it was expected that acetylthiocholine could not be hydrolyzed.[16] In a typical experiment, **S3** suspensions were incubated with a certain concentration of DFP and acetylthiocholine (1 mM). As shown in Figure 5, cargo delivery from the MS support can be finely tuned depending on DFP concentration. This result stresses again the role of the enzyme-based "control unit", which is able to "recognize" the presence of the inhibitor and consequently modulate the cargo delivered. Cargo delivery from **S3** can be modulated using concentrations of DFP as low as 5 µM. We also observed a similar response (payload release inhibition) with diethyl cyanophosphonate (DCNP), another acetylcholinesterase inhibitor (see Figure SI-5) and in a less extent with diethyl chlorophosphate (DCP) which indicated that cargo delivery can not only be regulated based on the amount of inhibitor but also on the inhibitor structure.

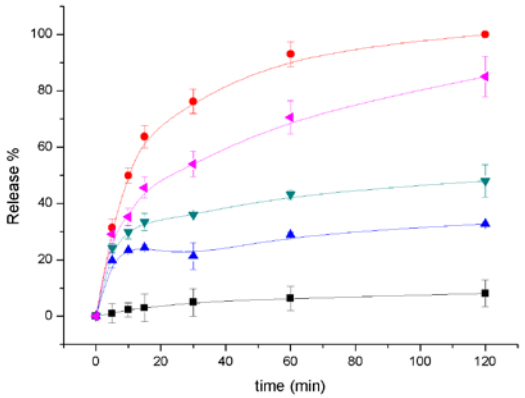

Figure 5. Normalized cargo release from **S3** determined by measuring safranin O fluorescence at 585 nm (λexc = 520 nm) versus time in aqueous solution (50 mM sodium phosphate buffer, pH 7.5) in the absence (black) and in the presence of acetylthiocholine 1 mM previously incubated with DFP 0.5 mM (blue), 0.05 (green), 0.005 mM (magenta) and without DFP (red).

Finally, we evaluated the performance of the nanodevice at cellular level. For this purpose, the human cervix adenocarcinoma (HeLa) cell line was used. First, in order to assess the biocompatibility of **S3** and discard any toxicity associated with the Janus scaffold or the coating shell, cell viability assays were carried out. Cells were incubated with different **S3** concentrations and evaluated by WST-1 cell viability assays after 24 h of exposure. The results demonstrated that **S3** nanoparticles were well-tolerated by HeLa cells at concentrations as high as 200 µg·mL^{-1} (see Figure SI-6). Next, the intracellular delivery of the cytotoxic agent doxorubicin using **S3$_{DOX}$** was studied. Doxorubicin is used in cancer therapy in order to kill cancer cells by DNA intercalation and oxidative stress. Cell were treated with 50 and 100 µg·mL^{-1} **S3$_{DOX}$** for 30 min, washed to remove non-internalized nanoparticles and further incubated with and without acetylthiocholine for 24 h. At lower **S3$_{DOX}$** dosage (50 µg·mL^{-1}), no reduction in cell viability was observed in the absence of acetylthiocoline whereas 20% cell death was induced in the presence of the stimulus (see Figure 6). At higher **S3$_{DOX}$** dosage (100 µg·mL^{-1}), cell viability decreased to around 65% in the absence of acetylthiocholine and it was further decreased to a remarkable 15% in the presence of acetylthiocholine (see also Figure 6). A more efficient elimination of cancer cells was achieved when **S3$_{DOX}$** and acetylthiocholine were co-administered. We also checked that acetylthiocholine did not have any toxic effect by itself. These results demonstrated that cargo release from the Janus nanodevice triggered by

This journal is © The Royal Society of Chemistry 20xx

Please do not adjust margins

acetylthiocholine also works in cells which is a complex high competitive medium.

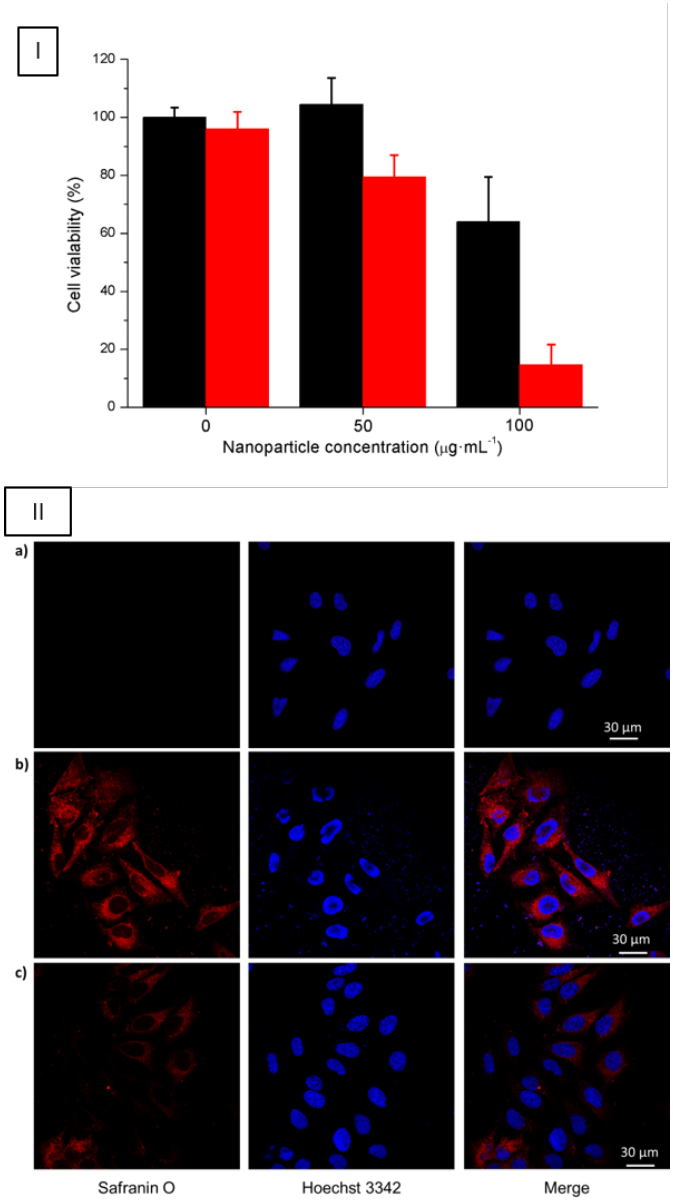

Figure 6. Cell experiments. Top (I): Cell viability assays of HeLa cells treated with different concentration of $\mathbf{S3}_{DOX}$ (0, 50 and 100 μg·mL^{-1}) in the absence (black bars or in the presence (red bars) of acetylthiocholine (40 mM). Three independent experiments were done. Data are expressed as mean ± σ. Down (II): Controlled release from **S3** (100 μg·mL^{-1}) in HeLa cells examined by confocal microscopy for (a) control experiment, (b) incubation with **S3** and acetylthiocholine (40 mM) and (c) incubation with **S3**. From left to right: cargo (safranin O) fluorescence, DNA-marker (Hoechst 3342) fluorescence and combined (merge).

Additionally, we carried out confocal microscopy experiments to directly image the payload release from the nanodevice in HeLa cells. For this experiments, HeLa cells were incubated with **S3** (100 μg·mL^{-1}) in the presence or in the absence of acetylthiocholine. For visualization, cells were stained with DNA-associated dye Hoeschst 3342 and intracellular release of **S3** was monitored by measuring safranin-associated fluorescence. As shown in Figure 6, a strong safranin-associated fluorescence was observed upon addition of acetylthiocholine due to the enzyme-mediated uncapping of the particles. On the other hand, only a slight safranin-fluorescence was observed in the absence of acetylthiocholine due to a partial rupture of the disulphide bond by the reductive environment inside the cells. These results were in agreement with WST-1 cell viability assays, thus confirming a much more efficient delivery of the cargo into cancer cells using the nanodevice in combination with acetythiocholine.

Regarding redox-responsive systems, various examples have been designed in the past years with the aim of improving the delivery of drugs into cancer cells. In fact, it has been shown that the incorporation of redox-sensitive moieties in the structure of doxorubicin-loaded biodegradable micelles improved tumour growth inhibition *in vivo*.[17] Other authors have developed glutathione-sensitive bowl-shaped polymeric nanomotors by introducing a disulphide bridge between hydrophilic poly(ethylene glycol) and hydrophobic polystyrene blocks and showed the intracellular delivery of doxorubicin in HeLa cells.[18] Also recently, polymeric nanoparticles containing disulphide bonds between their network have been developed and tested in cells and tumour models.[19] Inorganic materials containing disulphide bridges in their structure or capped with redox-responsive moieties able to realize controlled release of drugs have also been reported.[20] These recent studies point out the current interest in developing redox-sensitive delivery systems with optimized design in order to of achieve a better efficiency in drug delivery. As we have shown here, the incorporation of enzymes in combination with redox-responsive systems is a suitable strategy to modulate the delivery of gated nanodevices. In addition, the presence of gold nanoparticles could be of interest for future applications in which drug delivery is combined with optical hyperthermia.[21]

Conclusions

In summary, we reported here the design, synthesis and characterization of a new enzyme-controlled SS-OEG-gated nanodevice based on Janus Au-MS nanoparticles for cargo delivery. In particular, the Au-MS nanoparticles were functionalized with acetylcholinesterase enzyme on the Au-face and with disulfide-containging oligo(ethylene-glycol) chains on the MS face. Hydrolysis of acetylthiocholine by the enzyme resulted in the formation of thiocholine that induced cleavage of the disulfide bond in SS-OEG, uncapping of the pores and cargo delivery. The nanodevice was opened in the presence of acetylthiocholine but not acetylcholine, which demonstrates how the assembly of enzymes and molecular gates can synergically recognise small differences between molecules. Additionally, we found that the kinetics and amount of payload delivered can be finely tuned by the presence of enzyme inhibitors. Finally, the nanodevice, tested in cancer cells, displayed an enhanced cargo delivery (safranin O and doxorubicin) upon addition to the culture media of acetylthiocholine. Given the number of enzyme-mediated

Please do not adjust margins

redox processes[22] and gated ensembles that can be brought together in Janus Au-MS supports, we believe our findings could help in the development of new advanced delivery systems.

Acnowledgements

A. Llopis-Lorente thanks "La Caixa" Banking Foundation for his PhD fellowship. A. García-Fernández is grateful to the Spanish government for an FPU grant. The authors are grateful to the Spanish Government (MINECO Projects MAT2015-64139-C4-1, CTQ2014-58989-P and CTQ2015-71936-REDT) and the Generalitat Valencia (Project PROMETEOII/2014/047) for support. The Comunidad de Madrid (S2013/MIT-3029, Programme NANOAVANSENS) is also gratefully acknowledged.

References

1 a) E. Aznar, M. Oroval, L. Pascual, J. R. Murguía, R. Martínez-Máñez and F. Sancenón, *Chem. Rev.*, 2016, **116**, 561; b) S. Giret, M. Wong Chi Man and C. Carcel, *Chem. Eur. J.*, 2015, **21**, 13850; c) M. Vallet-Regí, F. Balas and D. Arcos, *Angew. Chem. Int. Ed.* 2007, **46**, 7548; d) K. T. Kim, S. A. Meeuwissen, R. J. M. Nolte and J. C. M. van Hest, *Nanoscale*, 2010, **2**, 844; e) G. Bao, S. Mitragotri and S. Tong, *Annu. Rev. Biomed. Eng.* 2013, **15**, 253; f) S. Mura, J. Nicolas and P. Couvreur, *Nat. Mater.*, 2013, **12**, 991; g) S.-H. Wu, Y. Hung and C.-Y. Mou, *Chem. Commun.*, 2011, **47**, 9972.

2 a) N. Kamaly, B. Yameen, J. Wu and O. C. Farokhzad, *Chem. Rev.*, 2016, **116**, 2602; b) Y. Li, G. Liu, X. Wang, J. Hu and S. Liu, *Angew. Chem. Int. Ed.*, 2016, **55**, 1760; c) N. K. Sharma, K. Neeraj and V. Kumar, *Drug Delivery Lett.*, 2014, **4**, 12; d) I. K. Yazdi, A. Ziemys, M. Evangelopoulos, J. O. Martinez, M. Kojic and E. Tasciotti, *Nanomedicine*, 2015, **10**, 3057; e) N. Z. Knežević and J.-O. Durand, *Nanoscale*, 2015, **7**, 2199.

3 a) L. K. E. A. Abdelmohsen, M. Nijemeisland, G. M. Pawar, G.-J. A. Janssem, R. J. M. Nolte, J. C. M. van Hest and D. A. Wilson, *ACS Nano*, 2016, **10**, 2652; b) M. Nijemeisland, L. K. E. A. Abdelmohsen, W. T. S. Huck, D. A. Wilson and J. C. M. van Hest, *ACS Cent. Sci.*, 2016, **2**, 843; c) X. Ma, A. Jannasch, U.-R. Albrecht, K. Hahn, A. Miguel-López, E. Schäffer and S. Sánchez, *Nano Lett.*, 2015, **15**, 7043; d) X. Ma, Ana C. Hortelao, A. Miguel-López and S. Sánchez, *J. Am. Chem. Soc.*, 2016, **138**, 13782; e) S. Sengupta, K. K. Dey, H. S. Muddana, T. Tabouillot, M. E. Ibele and P. J. Butler, A. Sen, *J. Am. Chem. Soc.*, 2013, **135**, 1406.

4 a) F. Tang, L. Li and D. Chen, *Adv. Mater.* 2012, **24**, 1504; b) Z. Li, J. C. Barnes, A. Bosoy, J. F. Stoddart and J. I. Zink, *Chem. Soc. Rev.*, 2012, **41**, 2590; c) D. Tarn, C. E. Ashley, M. Xue, E. C. Carnes, J. I. Zink and C. J. Brinker, *Acc. Chem. Res.*, 2013, **46**, 792; d) Y. Zhao, J. L. Vivero-Escoto, I. I. Slowing, B.G. Trewyn and V. S.-Y. Lin, *Expert Opin. Drug Deliv.*, 2010, **7**, 1013; e) C. Argyo, V. Weiss, C. Bräuchle and T. Bein, *Chem. Mater.*, 2014, **26**, 435; f) Y.-W Yang, Y.-L. Sun and N. Song, *Acc. Chem. Res.*, 2014, **47**, 1950; g) A. Popat, S. B. Hartono, F. Stahr, J. Liu, S. Z. Qiao and G. Qing Lu, *Nanoscale*, 2011, **3**, 2801.

5 a) T. M. Guardado-Alvarez, L. S. Devi, M. M. Russell, B. J. Schwartz and J. I. Zink, *J. Am. Chem. Soc.*, 2013, **135**, 14000; b) F. Sancenón, L. Pascual, M. Oroval, E. Aznar and R. Martínez-Máñez, *ChemistryOpen*, 2015, **4**, 418; c) A. Baeza, E. Guisasola, E. Ruiz-Hernández and M. Vallet-Regí, *Chem. Mater.* 2012, **24**, 517; d) Z. Zhang, D. Balogh, F. Wang, S. Y. Sung, R. Nechushtai and I. Willner, *ACS nano*, 2013, **7**, 8455; e) A. Bansal and Y. Zhang, *Acc. Chem. Res.*, 2014, **47**, 3052; f) C. Coll, A. Bernardos, R. Martínez-Máñez and F. Sancenón, *Acc. Chem. Res*., 2013, **46**, 339; g) Y. Chen, H. Zhang, X. Cai, J. Ji, S. He and G. Zha, *RSC Adv*., 2016, **6**, 92073. h) C. Giménez, E. Climent, E. Aznar, R. Martínez-Máñez, F. Sancenón, M. D. Marcos, P. Amorós and K. Rurack, *Angew. Chem. Int. Ed.*, 2014, **53**, 12629. i) A. Llopis-Lorente, B. Lozano-Torres, A. Bernardos, R. Martínez-Máñez and F. Sancenón, *J. Mater. Chem. B*, 2017, **5**, 3069.

6 a) P. Díez, A. Sánchez, M. Gamella, P. Martínez-Ruíz, E. Aznar, C. De La Torre, J. R. Murguía, R. Martínez-Máñez, R. Villalonga and J. M. Pingarrón, *J. Am. Chem. Soc.*, 2014, **136**, 9116. b) R. Villalonga, P. Díez, A. Sánchez, E. Aznar, R. Martínez-Máñez and J. M. Pingarrón, *Chem. Eur. J.*, 2013, **19**, 7889. c) A. Llopis-Lorente, P. Díez, A. Sánchez, M. D. Marcos, F. Sancenón, P. Martínez-Ruiz, R. Villalonga and R. Martínez-Máñez, *Nat. Commun.*, 2017, **8**, 15511.

7 a) C. Gotti and F. Clementi, *Prog. Neurobiol.*, 2004, **74**, 363; b) J. Lindstrom, *Mol. Neurobiol*., 1997, **15**, 193; c) L. Descarries, V. Gisiger and M. Steriade, *Prog. Neurobiol.*, 1997, **53**, 603.

8 H. C. Froede and I. B. Wilson, *J. Biol. Chem.*, 1984, **259**, 11010.

9 a) J. A. Turkevich, *Discuss. Faraday Soc.*, 1951, **11**, 55; b) G. Frens, *Nature*, 1973, **241**, 20.

10 P. Tengvall, E. Jansson, A. Askendal, P. Thomsen and C. Gretzer, *Colloids Surf. B*, 2003., **28**, 261.

11 A. Sánchez, P. Díez, P. Martínez-Ruíz, R. Villalonga and J. M. Pingarrón, *Electrochem. commun.*, 2013, **30**, 51.

12 S. Brunauer, P. H. Emmett and E. Teller, *J. Am. Chem. Soc*., 1938, **60**, 309.

13 E. P. Barrett, L. G. Joyner and P. P. Halenda, *J. Am. Chem. Soc.*, 1951, **73**, 373.

14 a) G. L. Ellman, K. D. Courtney, V. Andres and R. M. Featherstone, *Biochem. Pharmacol*., 1961, **7**, 88; b) P. Nagy, *Antioxid. Redox Signal.*, 2013, **18**, 1623; c) P. C. Jocelyn, *Methods Enzymol.*, 1987, **143**, 246.

15 a) R. A. Westsmith and R. E. Abernethy, *AMA Arch. Ophthalmol.*, 1954, **52**, 779; b) K. Kim, O.G. Tsay, D.A. Atwood and D.G. Churchill, *Chem. Rev.*, 2011, **111**,5345.

16 a) T.M. Shit, R.K. Kan and J.H. McDonough, *Chem. Biol. Interact.,* 2005, **157**, 293; b) C. H. Gunderson, C. R. Lehmann, F. R. Sidell and B. Jabbari, *Neurology*, 1992, **42**, 946; c) A. Silver, The Biology of Cholinesterases, *Elsevier*, New York, 1974, 449-488.

17 Y. Zhu, J. Zhang, F. Meng, C. Deng, R. Cheng, J. Feijem and Z. Zhong, *J. Control. Release*, 2016, **233**, 29.

18 Y. Tu, F. Peng, P. B. White and D. A. Wilson, *Angew. Chem. Int. Ed.*, 2017, **56**, 7620.

19 a) J. Sun, Y. Liu, Y. Chen, W. Zhao, Q. Zhai, S. Rathod, Y. Huang, S. Tang, Y. Tae Kwon, C. Fernandez, R. Venkataramanan and S. Li, *J. Control. Release*, 2017, **258**, 43; b) W. C. de Vries, D. Grill, M. Tesch, A. Ricker, H. Nüsse, J. Klingauf, A. Studer, V. Gerke and B. J. Ravoo, *Angew. Chem. Int. Ed.*, 2017, DOI: 10.1002/anie.201702620.

20 a) J.T. Lin, Z.-K. Liu, Q.-Lin Zhu, X.-H. Rong, C.-L. Liang, J. Wang, D. Ma, J. Sun, and G.-H. Wang, *Colloids Surf. B*, 2017, **155**, 41; b) L. Han, X.-Y. Zhang, Y.L. Wang, X. Li, X.-H. Yang, M. Huang, K. Hu, L.-H. Li and Y. Wei, *J. Control. Release*, 2017, DOI: 10.1016/j.jconrel.2017.03.018; c) Q. Zhang, C. Shen, N. Zhao and F.-J. Xu, *Adv. Funct. Mater.*, 2017, **27**, 1606229; d) S. Zhao, M. Xu, C. Cao, Q. Yu, Y. Zhou and J. Liu, *J. Mater. Chem. B.*, 2017, DOI:10.1039/C7TB00613F.

21 J. F. Hainfeld, L. Lin, D. N. Slatkin, F. A. Dilmanian, T. Vadas and H. M. Smilowitz, *Nanomedicine*, 2014, **10**, 1609.

22 D. Gamenara, G. Seoane, P. Saenz Mendez and P. Dominguez de Maria, Redox Biocatalysis: Fundamentals and Applications, *John Wiley & Sons*, 2012.

 This journal is © The Royal Society of Chemistry 20xx

Please do not adjust margins